Chemie der Erde 77 (2017) 535–544

Contents lists available at ScienceDirect

Chemie der Erde

journal homepage: www.elsevier.de/chemer

Cyanobacterial mineralisation of posnjakite ($Cu_4(SO_4)(OH)_6{\cdot}H_2O$) in Cu-rich acid mine drainage at Yanqul, northern Oman

Bernhard Pracejus[a,*], Aliya Al-Ansari[b], Huda Al-Battashi[b]

[a] Department of Earth Science, P.O. Box 36, 123 Al-Khoud, Muscat, Oman
[b] Department of Biology, Sultan Qaboos University, P.O. Box 36, 123 Al-Khoud, Muscat, Oman

ARTICLE INFO

Article history:
Received 21 December 2016
Received in revised form 29 April 2017
Accepted 8 June 2017
Editorial handling - Alexander Deutsch

Keywords:
Posnjakite
Biomineralisation
Cyanobacteria
Acid mine drainage
Remediation

ABSTRACT

This is the first detailed account of the copper sulfate posnjakite ($Cu_4(SO_4)(OH)_6{\cdot}H_2O$) coating cm-long filaments of a microbial consortium of four cyanobacteria and *Herminiimonas arsenicoxydans*. It was first observed on immersed plant leaves and stalks in a quarry sump of the abandoned Yanqul gold mine in the northern region of Oman; rock surfaces in the immediate vicinity show no immediate evidence of posnjakite. However, a thin unstructured layer without filaments but also containing the brightly coloured turquoise posnjakite covers ferruginous muds in the sump. Although copper is a potent bactericide, the microbes seem to survive even at the extreme heavy metal concentrations that commonly develop in the sump during the dry season ($Cu^{2+} \approx 2300$ ppm; $Zn^{2+} = 750$ ppm; $Fe^{2+} \approx 120$ ppm; $Ni^{2+} = 37$ ppm; $Cr_{total} = 2.5$ ppm; $Cl^- = 8250$ ppm; and $SO_4^{2-} = 12{,}250$ ppm; pH ~2.6), thus leading to the precipitation of posnjakite over a large range of physicochemical conditions. Upon exposure to the prevailing arid climate, dehydration and carbonation quickly replace posnjakite with brochantite ($Cu_4(SO_4)(OH)_6$) and malachite ($Cu_2(CO_3)(OH)_2$). To characterise and understand the geochemical conditions in which posnjakite precipitates from undersaturated fluids (according to our thermodynamic modelling of the dominant elements), waters from rainy and dry periods were analysed together with various precipitates and compared with the observed field occurrences. The findings imply that posnjakite should not form in the examined environment through purely inorganic mechanisms and its origin must, therefore, be linked to the encountered microbial activities.

1. Introduction

Situated in the Samail ophiolite (obducted continental crust) of northern Oman, the abandoned Yanqul gold mine (23°40′40.79″N; 56°32′27.35″E) was established in a belt of mafic rocks (basalts) that contain numerous Cyprus-type copper-rich volcanogenic massive sulfide (VMS) deposits (Fig. 1; Hannington, 1993; Galley et al., 2007). Once the gold and copper production at the Yanqul deposit ceased, the open pits collected occasional rain and ground waters that had reacted with the relict metal sulfides of the surrounding rocks. Onsetting ore mineral oxidation resulted in a strong acidification of the waters through the formation of sulfuric acid (e.g., Chavéz, 2000; Essalhi et al., 2011), thus intensifying further oxidation and dissolution processes (industrially induced enhanced gossan development in the open quarry) and mobilising significant quantities of base metals. Drainage focused these acidic and metal-laden fluids in the quarry sumps (lowest part of the mine), where various mineralisation and/or dissolution processes occur continuously, depending on strongly changing water availability during dry and "rainy" seasons and large ambient temperature fluctuations, respectively.

During a sampling campaign collecting waters and secondary copper minerals, conspicuously coloured precipitates enveloping centimeter-long microbial filaments were observed on the edge of one of the mining sumps; we later identified these mineralised coatings as posnjakite ($Cu_4(SO_4)(OH)_6{\cdot}H_2O$). Similar turquoise precipitates had previously been noted by the first author in inaccessible places of the same sump and in a Zambian copper mine (Fitwaola mine) but had not been sampled. The detailed genetic identification of the microbial consortium is subject of a separate paper by Al-Ansari et al. (in preparation), but we report here that up to 4 different cyanobacterial species plus *Herminiimonas arsenicoxydans* seem to be present.

Although the role of microbes in mineralisation and mobilisation processes has been investigated for some time in the context of almost any conceivable element (Walter et al., 1972; Pan-Hou and Imura, 1981; Kretzschmar, 1982; Vuorinen et al., 1983; Wood and Wang, 1983; Zierenberg and Schiffman, 1990; Anderson and Lovley,

* Corresponding author.
E-mail address: pracejus@squ.edu.om (B. Pracejus).

http://dx.doi.org/10.1016/j.chemer.2017.06.001
0009-2819/

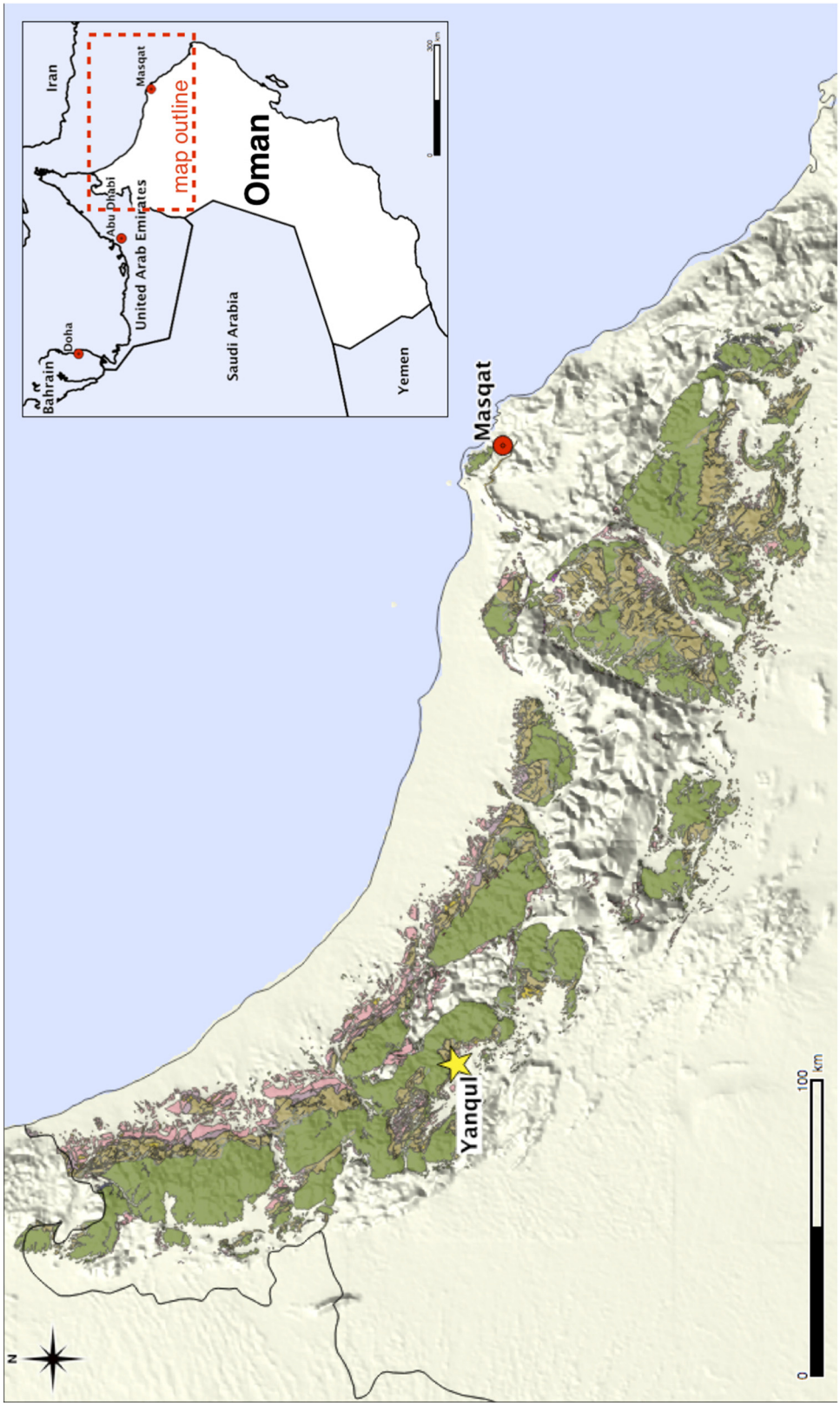

Fig. 1. Northern Oman with its coastal mountain chain is the host of an ophiolite system containing numerous volcanogenic massive sulfide (VMS) deposits within mafic rocks; the Yanqul gold mine (asterisk; 23°40′40.79″N; 56°32′27.35″E) belongs to these deposits. The green/olive-coloured regions reflect the distribution of mantle (ultramafic) rocks, while the pink areas illustrate the spread of crustal (mafic) rocks. The map was produced with SimpleDEMViewer for Mac (version 4.4.9), ASTER GDEM data (product of METI and NASA), QGIS (version 2.0.1-Dufour) under GNU General Public License, and the geological map of Oman (Béchennec et al., 1993).

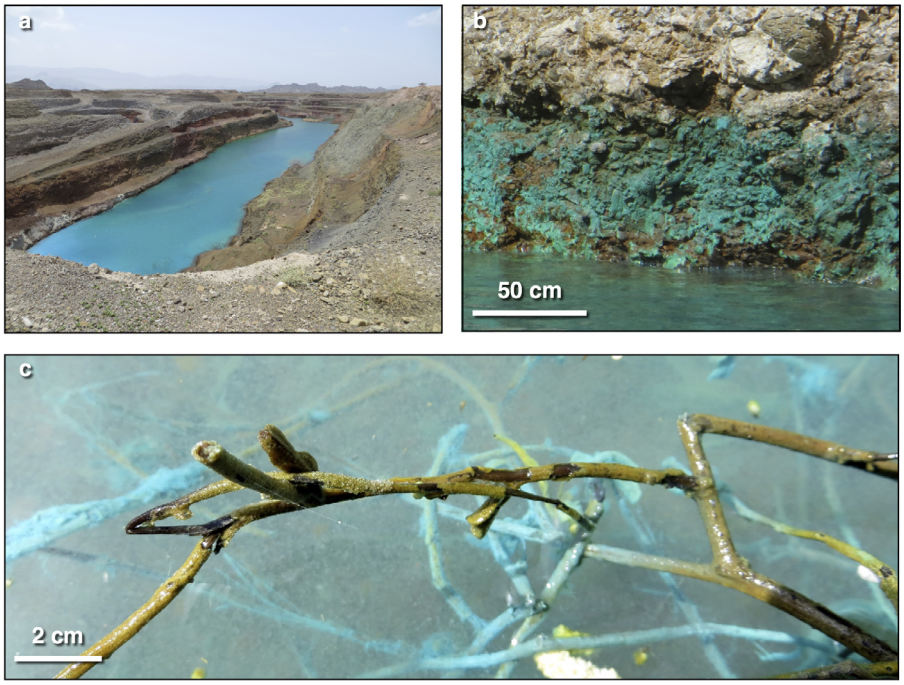

Fig. 2. a The blue water of the Yanqul quarry sump implies the presence of high concentrations of dissolved copper (plus other base metals; see analytical section); the pond is approximately 300 m long. b Evaporating Cu-rich waters have left a green mm-thick and ~50 cm wide layer of secondary copper minerals rimming the Yanqul quarry sump. c Decomposing plant stalks and leafs provide the substrate for microbial growth in the Yanqul quarry sump.(For interpretation of the references to colour in this figure legend, the reader is referred to the web version of this article.)

2002; Douglas, 2004; Shuster et al., 2014; Jiang et al., 2015, 2017), extreme habitats, such as the location described in this paper, shift the boundaries of life into evermore unlikely settings for biogenesis (origin of life) at 'the interface of the pre-biotic and biotic worlds' (Greenwood Hansma, 2010; Cleaves et al., 2011; Longo and Blaber, 2012; Li et al., 2013) and demonstrate that life must have influenced the development of our "inorganic" early planet to a much larger degree than previously assumed (Hazen and Ferry, 2010; Corenblit et al., 2011).

The extreme habitats mentioned above include elevated temperatures in marine hydrothermal systems (Pracejus and Halbach, 1996; Dekov et al., 2013), highly saline fluids (Oren, 1994), and toxic environments rich in heavy metals (Bednar et al., 2005; Edraki et al., 2005; Courtin-Nomade et al., 2009; Davies et al., 2011). Elements, such as copper and silver, are bactericides (Trevors, 1987; Abinaya et al., 2016) and seemingly would inhibit microbial existence. A joint effect of the latter elements with highly acidic fluids (acid mine drainage; AMD) would then render conditions for microbial survival (and possible biomineralisation processes) even more unlikely. Yet, the presence of posnjakite-coated cyanobacterial filaments in the copper-laden acid mine drainage at Yanqul (and probably elsewhere) attests to the fact that cyanobacteria, which often live in alkaline to neutral waters (Brito et al., 2017; Genuário et al., 2017), have indeed found ways of coping with this particular stress – Little is known about their occupancy of acidic environments and even less about surviving copper toxicity.

Since extremophiles developed many strategies countering negative environmental effects (Averhoff and Müller, 2010; Peeples, 2014), their respective habitats need to be thoroughly characterised physicochemically and biochemically in order to better understand biomineralisation and biomobilisation processes. Therefore, this paper applies a broad multidisciplinary approach to show how the posnjakite can precipitate from an undersaturated solution through cyanobacterial activities. The findings may, on one hand, be useful for AMD remediation (Díaz-Tena et al., 2013; Pracejus and Moraetis, 2015) while, on the other hand, they may also shed light on environments mimicking early life forms on Earth or even extraterrestrial conditions in which life might be harboured (Panda et al., 2015).

2. Methods

2.1. Sampling and sample treatment

The collected materials consist of two sample types:

- Biological substrates (decomposing plant matter submerged in the quarry sump), on which the filaments were attached. The sample was directly placed in a sterile plastic bag and then detached from the main stem of the plant without contact to hands or tools. On return to the lab, the sample was kept in the fridge until its further handling.
- Evaporitic crusts of secondary sulfates and carbonates were collected as well, because microbial remains, although anticipated, could not be detected in the field. These materials were first air-dried, then placed on a hotplate (over night at 50 °C) to remove further moisture, and embedded in an epoxy resin for the preparation of polished rock sections (Araldite; compare also Section 2.2 for additional information).

2.2. Optical and scanning electron microscopy (SEM), microanalysis (EDS)

- Wet microbial filaments were cut off, placed on a microscope slide, covered with a thin glass plate, and viewed in transmitted light under a Zeiss Axioplan optical microscope.
- Araldite-embedded rock substrate blocks were cut to size, ground, and polished on one plain with 1 μm diamond powder to be observed in reflected light under the same microscope (necessary to also identify small opaque mineral grains that could have been important for the overall understanding of the mineralisation).

- Dried filaments were mounted on an aluminium sample holder, coated with carbon, and then inspected under the SEM (JEOL Field Emission Scanning Electron Microscope JSM-77600F; 20 keV, 76 μA, working distance 8 mm, probe current 8 A).
- Geochemical spot analyses of the mineral coatings from the microbial strands were performed with an EDS system (Oxford Instruments; solid state detector, AZtech v. 2.0 software, INCA) for their element composition.

2.3. Mineralogy (X-ray diffraction/XRD)

A sub-sample of the coated filaments was dried and placed on a spinning single-crystal silicon sample holder in the X′Pert PRO X-ray Diffractometer (Panalytical) used Cu-Kα radiation (1.54060 Å). The machine was set to 40 mA and 45 kV, and measured at a step size of 0.0167°2ϑ. The obtained mineral peaks were then evaluated with the help of the "High Score Plus" software.

2.4. Hydrochemistry

Eh, pH, and temperature measurements were made with a portable instrument (hand-held Mettler Toledo SG2) in the quarry sump to identify the in-situ physicochemical parameters governing precipitation processes in the metal-rich fluids. A portable photometer (LaMotte Smart 2 Colorimeter; Cr #3645-0.00-1.00 ppm; Cu #3646-0.00-6.00 ppm, Fe #3648-0.00-6.00 ppm, Si #3664-0.0-4.0 ppm, Sulfate #3665-0-100 ppm), direct titration (LaMotte; Chloride #3643-0-max ppm), and colorimetric test kits (LaMotte Mn #3588-02-0.05-1.00 ppm; Ni #7802-0.5-10 ppm; Zn #7391/02-0-10 ppm) were used in the field, all chemical measurements were repeated in the lab for improved analytical conditions. All tests are laid out for sub-ppm- to ppm-levels (drinking water monitoring), many samples had to be diluted fairly strongly prior to analysis. Thus, an estimated additional analytical error of ±10% could be expected.

2.5. Experimental investigations

Mimicking field conditions in the quarry sump, a laboratory experiment was conducted to determine the possibility of cultivating the collected microbes and precipitating posnjakite from a Cu-carrying solution. In a sterile conical flask, 200 ml of the sterilised Cu-rich fluid together with the palm fibers were first inoculated with the original sample. Then, the experiment was kept in the lab on a slowly moving shaker to establish microbial growth on the fibers for 3 months, after which it was transferred to a roof-top position for a final sun exposure over 3 weeks. The experimental conditions were as follows:

- Dissolving sterilised $CuSO_4{\cdot}5H_2O$ in freshly produced distilled water, a sterile solution of 2000 ppm Cu was prepared,
- High acidity (pH ~ 2.5) was attained through an addition of sulfuric acid,
- The temperature in the laboratory was fairly constant at ~20 °C, while outdoor exposure of the experiment to the sun resulted in temperatures of up to 42 °C,
- Slowly decomposing sterile palm wood fibers were the sole source of nutrients and also served as substrate for microbial filaments.

2.6. Thermodynamic modelling

Thermodynamic stability fields for solids and mine waters according to measured field data were calculated and plotted with the "Act2" module from "The Geochemist's Workbench" (version 8.0; Bethke, 2008). All observed concentrations from the dry and "wet" seasons, 2013 and 2014, respectively, were included in the initial models to identify interdependencies between dissolved and mineralised species. In some cases, the thermodynamic calculations showed mineral species that have not been detected in the field, despite an extensive search that identified more than 50 secondary minerals. Thus, individual elements that led to this predicted formation of such unsubstantiated minerals were suppressed (excluded from the models) to match both field findings and final models as far as possible; this will be further explained in the modelling results section. The dissolved carbonate concentration was not measured but assumed to be close to that of normal surface waters (10-3 Mol/l; Brookins, 1988).

3. Results

3.1. Field observations

Already on first sight at various Yanqul quarry sumps, it becomes apparent that there must be a high mobility of copper (and assumedly other base metals) in the deposit area. The brightly coloured fluids optically stand out from the reddish brown oxidised surrounding rocks (gossan; Fig. 2a). This observation is also corroborated by a thin layer of blue-green precipitates along the pond edges, which marks a prevalence of copper minerals (Fig. 2b). On closer examination, the visited pond revealed extremely fine-grained and turquoise-coloured mineralisations in conjunction with decomposing plant stalks and leafs (Fig. 2c; compare also Fig. 3a). It is important to note that well-structured precipitates only occurred as coatings of cm-long microbial filaments, while finest crystallites within an unstructured but slightly cohesive layer (bacterial mat) without obvious filaments covers ferruginous muds in the sump, producing the strongly tinted turquoise pond with the typical posnjakite coloration.

The microscope shows fine crystallites rather than an amorphous mass on these filaments (Fig. 3b), either as a continuous layer, isolated aggregates or individual grains (Fig. 3c). Although most of the observed microbial strands appear as "spaghetti"-like smooth filaments, there are occasionally fibers that exhibit short thorn-like appendices (observed in the samples from both the pond and one sample from a vug of the surrounding rocks; Fig. 3d and e). Along with the filaments, a gelatinous substance resembling a mineralised gel (relict of a microbial mat?) that binds several cell structures was observed in the mentioned rock sample (Fig. 3f). A similar but much thicker and much more solid biofilm (~3 cm), which is also associated with Cu-precipitation, has been recovered from a different mining site and appears to be typical for a higher energy environment associated with running waters but is not discussed here any further. Morphological details of the microbial strands and the mineral coatings are presented in Fig. 4a-f. Important to mention here is the fact that there seem to be at least two kinds of filamentous organisms in the collected samples with vastly different filament diameters: Most coated fibers have a diameter of around 5 μm, while the finer ones (practically without mineralisation) show only ~0.5 μm (compare Fig. 4a, c and d).

3.2. Composition of filament coatings

Mineral deposits on the bacterial strands and secondary precipitates on the rocks were analysed by X-ray diffraction (XRD) and present a fairly simple mineralogy:

- Filament coatings are almost exclusively composed of posnjakite ($Cu_4(SO_4)(OH)_6{\cdot}H_2O$), exhibiting a very clear and distinctive spectrum; minor brochantite ($Cu_4(SO_4)(OH)_6$) and malachite ($Cu_2(CO_3)(OH)_2$) are also present,

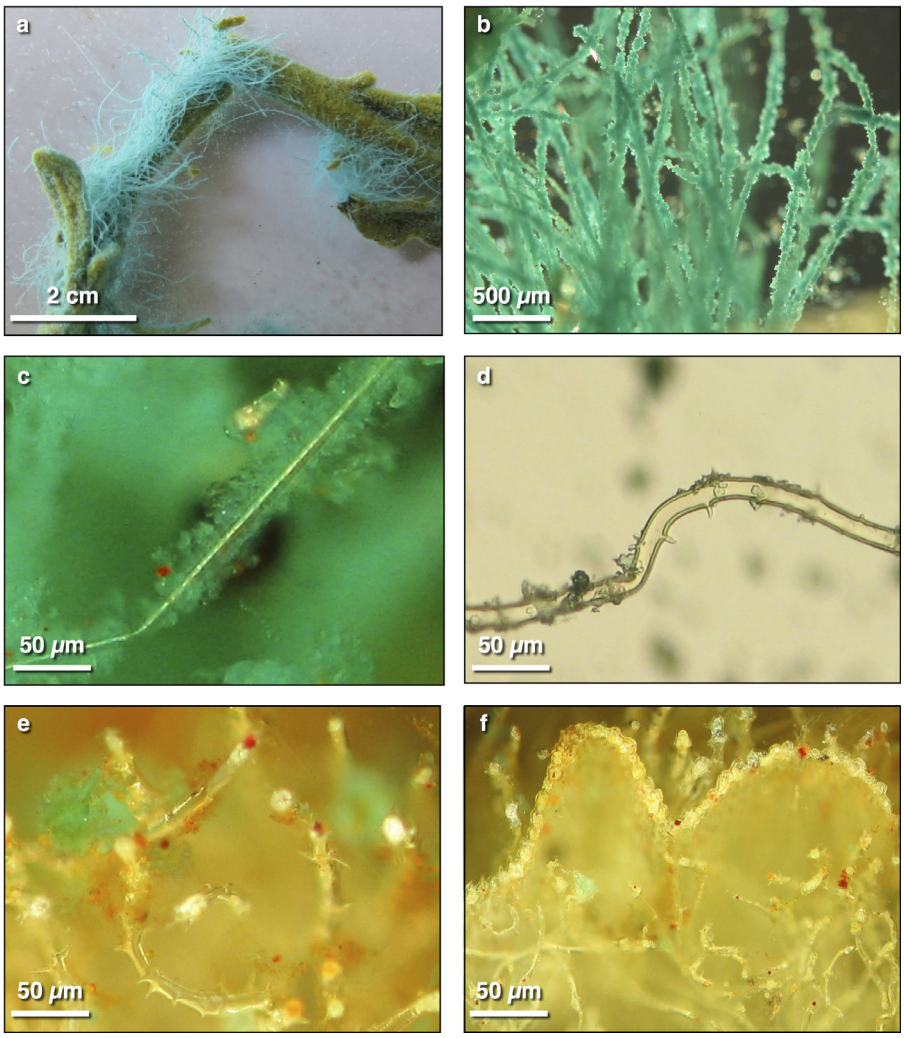

Fig. 3. a The sampled material (compare Fig. 2c) clearly shows long microbial filaments. b Under the microscope, fine crystallites become visible that coat the microbial filaments. c A polished section from the original sample shown in Fig. 3a, observed under reflected light and crossed polarisers. The microbial filament is clearly enveloped by posnjakite. d Higher magnification of the quarry sump microbes show a number of filaments that have short appendices; few isolated fine crystallites are also visible, observed under transmitted light. e A polished section of the rocks and precipitates from the edge of the pool contains the same microbial filaments with short appendices (compare previous photo of Fig. 3d), observed under reflected light and crossed polarisers. f Some parts of the filamentous aggregates contained in the rocks show portions of a gelatinous substance (microbial mat?) resembling a mineralised gel found in another location, observed under reflected light and crossed polarisers.

- Precipitates from rocks along the pool edges, on the other hand, are dominated by brochantite and malachite, while only subordinate posnjakite peaks exist.

Gypsum ($CaSO_4{\cdot}2H_2O$), although occasionally seen in some vugs of the materials described above, has neither been detected in these samples nor in the filament coating (this observation is important in the context of the mineral formation order). However, upon further increased evaporation of the sump fluids, cm-sized gypsum laths begin to coat submerged rocks and mud until these are more or less covered completely.

The geochemical microanalysis (EDS; Table 1) of the posnjakite filament coatings shows a composition dominated by copper (Cu), oxygen (O), and sulfur (S) with minor additions of silicon (Si) and aluminium (Al) and rarely some iron (Fe); hydrogen (H) cannot be measured by the instrument. Since carbon (from carbonates) was also not analysed by EDS because of the C-coating of the samples, excess Cu relative to S (~1/3 more Cu) when compared with the structure of pure posnjakite, may be explained by an admixture of malachite (XRD analysis confirms small amounts).

Table 1
Microanalysis (EDS) of microbial filaments; the structural formula was omitted (for comments refer to text); all values in wt.%.

Analysis #	Cu*	O	S	Al	Si	Fe	Sum
1	60.2	33.1	4.7	0.1	0.7	0.5	99.3
2	63.1	31.3	4.6	0.5	0.4	0.0	99.9
3	62.4	31.7	5.9	0.0	0.0	0.0	100.0
4	59.6	34.5	5.2	0.4	0.3	0.0	100.0
Average	61.3	32.7	5.1	0.3	0.4	0.1	99.8

The attempted calculation of the structural formula to confirm the mineralogy XRD analysis again showed an overabundance of copper, which may be attributed to the presence of brochantite and/or malachite as mentioned above. Since the posnjakite crystallites are very fine-grained and therefore highly reactive, the vacuum in the SEM sample chamber (together with the electron beam energy) may already suffice to start a dehydration of this mineral, resulting in the formation of brochantite or intermediate compounds.

Although there is a high abundance of other base metals in the pond from which the posnjakite precipitated, the mineral does

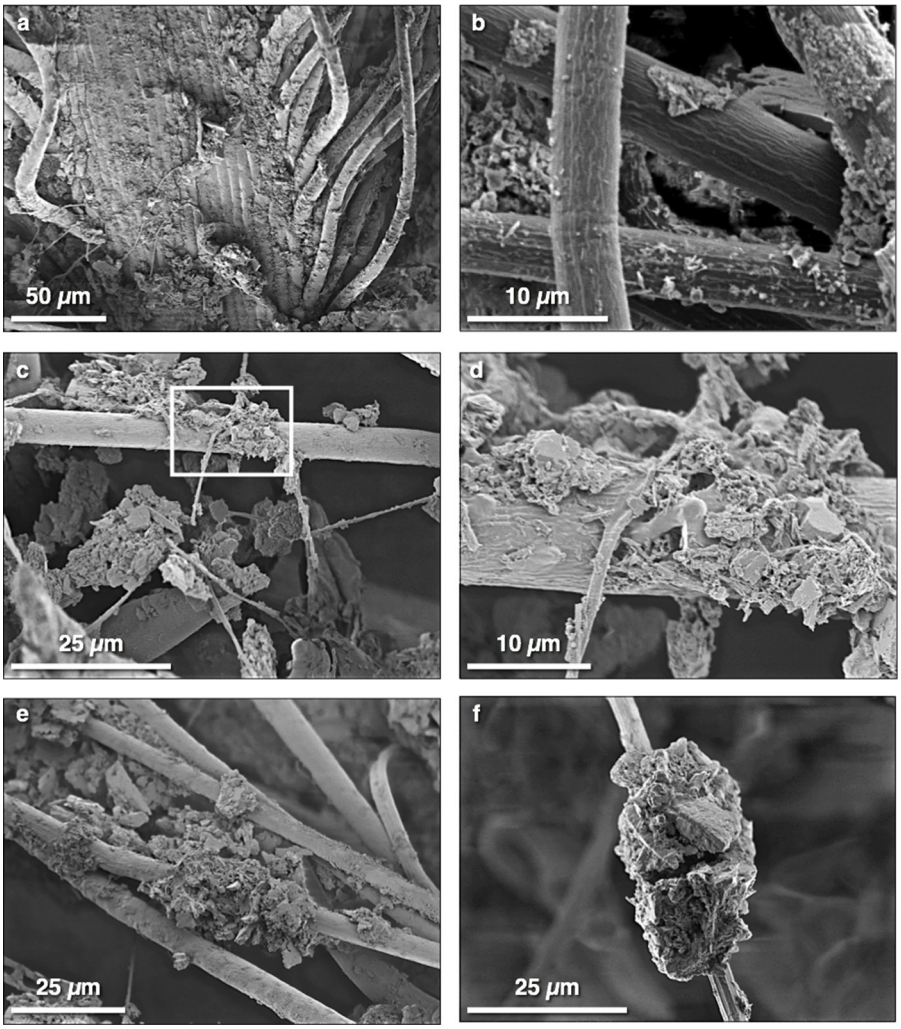

Fig. 4. a A striated leaf acts as base for the microbial filaments; SEM picture. b The enlargement shows the topography of the filaments and the partial Cu-rich coating; SEM picture. c The SEM picture displays two types of filaments with strongly differing diameters. Cu-rich precipitates cover filaments and occupy interstitial spaces; the frame relates to Fig. 5d. d Enlargement of previous SEM image. e Cu-rich precipitates on smooth microbial strands. f Cu-mineral aggregate on microbial strand.

not accommodate any of these in its structure. Iron, seen in one analysis, may have precipitated as a fine hydroxide particle but is generally not observed in these precipitates. The low silica values might be attributed to the microbial cell membranes, since various organisms utilise this element to increase the rigidity of their cell-walls (Engel, 1953; Holzapfel and Engel, 1954; Heinen, 1965; Walter et al., 1972; Juniper and Fouquet, 1988), while aluminium could be an artefact from the sample preparation.

3.3. Hydrochemistry and associated precipitates

The water sampling and testing during the dry season of May 2013 and after a prolonged wet season in April 2014 produced strongly varying geochemical characteristics of the collected fluids (Table 2) with highly elevated base metal, silica, sulfate, and chloride levels as well as a high oxidation potential together with the fairly low pH of 2.57 in the dry period. The following wet season replenished the pond and diluted the respective components to much lower values. However, when element abundances of the two seasons are compared (Fig. 5), it is evident that not only a dilution occurred between the two sample sets but that further precipitation reactions must have selectively reduced the concentrations of some of the elements, in particular, those of Cu^{2+} and Fe^{2+}.

Table 2
Yanqul mine water samples collected during dry season in May 2013 and after prolonged wet season of April 2014. Local surface water analysed as background information showed Eh 62 mV, pH 9.03 (typical for the region), slightly elevated concentrations of 1.3 ppm Cu, and <0.0 ppm Fe; for analytical precision see methods section.

	Units	Dry Season 2013	Wet Season 2014
pH		2.57	4.51
Eh	(mV)	573	343
T	(°C)	34.9	27.8
SO_4^{2-}	ppm	12,250	575
Cl^-	ppm	8250	280
Cu^{2+}	ppm	2280	7.2
Zn^{2+}	ppm	750	75
Si^{4+}	ppm	167.5	15.45
Mn^{2+}	ppm	150	25
Fe^{2+}	ppm	117	0.3
Ni^{2+}	ppm	37	1
Cr_{total}	ppm	2.5	0.02

Monitoring an evaporating fluid sub-sample from the dry season in the laboratory (at the *in situ* measured temperature) also substantiates the idea of a relatively strong sulfate decrease at the end of the dry season (such conditions are not shown for this context). Similar to what was already observed along the edge of the sump, gypsum also crystallised in the evaporating

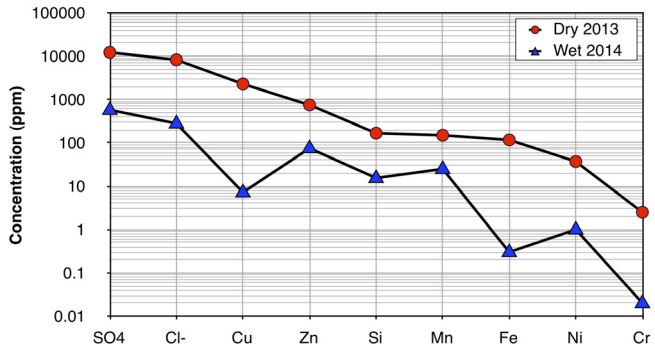

Fig. 5. When compared with the dry season, the concentration of dissolved elements measured in the fluids of the wet season, has dropped significantly.

dry-season fluid as the main mineral phase after the initial iron hydroxide precipitation. Only when the solution had almost completely dried up, further minerals appeared with a final mixture that did not contain posnjakite but rather chalcanthite ($CuSO_4{\cdot}5H_2O$) and Cu-pentahydrite ($(Mg_{0.49}Cu_{0.41}Mn_{0.08}Zn_{0.02})SO_4{\cdot}5H_2O$) as the Cu-carrying phases, while halotrichite ($FeAl_2(SO_4)_4{\cdot}22H_2O$) and alunogen ($Al_2(SO_4)_3{\cdot}17H_2O$) concentrated remaining iron and aluminium in the final sulfates.

3.4. Experimental posnjakite precipitation

The conducted experiments with the cultured cyanobacteria from Yanqul corroborate that posnjakite precipitation is highly substrate- and organism-specific: Relatively few coarse cyanobacterial strands developed the same coating as in the field (Fig. 6a), while the abundant finer cyanobacterial filaments, as well as the palm wood and the glass walls, were completely free of precipitates. Upon sun exposure, all filaments are easily identified as cyanobacteria through their prolific oxygen production (Fig. 6b). *Herminiimonas arsenicoxydans* plays no role in this setting (its short rod-shape cells would not aggregate into the observed large filamentous cell structures). It may, however, benefit from the Cu-reduced environment around the cyanobacterial cells.

3.5. Thermodynamic modelling

To improve our understanding of the microbe-mediated precipitation of posnjakite ($Cu_4(SO_4)(OH)_6{\cdot}H_2O$) from undersaturated fluids, we modelled the components on an inorganic basis and at the conditions observed during the dry season in 2013, when the microbial assemblage was collected (Table 2; Fig. 7a and b; Bethke, 2008), as well as for the "wet" season in 2014. However, the physicochemical conditions in the dry season, during which the filament coatings were collected, offer more clues to the precipitational environment of posnjakite than those of the "wet" season, because the respective mineral stability fields are larger due to the much higher concentrations of the dissolved metals; the "wet" season is not considered further.

Arsenic, which can be a significant accessory element in some sulfide deposits, does not play an important role in the examined Cu-rich system (only one small mineral sample containing scorodite – $FeAsO_4{\cdot}2H_2O$ – has been observed so far in this location). Therefore, we excluded Cu-sulfarsenates, such as arsentsumebite, arthurite, chalcophyllite, gartrellite, leogangite, and parnauite from our modelling considerations (Frost et al., 2011).

Since iron plays an important role in the examined systems, its stability is examined first for the displayed acid to intermediate pH range (0–6; Fig. 7a). Initially, and without considering dissolved Cu and Cr, oxic environments dominate with relatively large stability fields for dissolved iron sulfate species ($FeSO_4^+$ and $FeSO_{4(aq)}$ and hematite (Fe_2O_3)), while pyrite (FeS_2) covers the reducing space. If Cu and Cr species were also included in the model, additional fields for delafossite ($CuFeO_2$) and chromite ($FeCr_2O_4$) would appear over large parts of hematite and iron sulfate stabilities. However, there is no evidence for the formation of these minerals in Yanqul, despite an extensive search in the field, probably indicating retardation processes. Thus, these minerals are excluded from further considerations. The water, from which the microbial assemblage was collected, plots close to the boundary with $FeSO_{4(aq)}$ within the hematite stability field, indicating the ongoing precipitation of iron oxides/hydroxides that is corroborated by field and laboratory evidence.

In the copper stability diagram, dissolved species also spread over large portions of the shown pH range (Fig. 7b). Cu^{2+} dominates here, while the monovalent and strongly temperature dependent $CuCl_2^-$ (<28 °C it becomes unstable in the wet season scenario) is less important at lower oxidation potentials but still above sulfide stabilities, where covellite (CuS) and chalcocite (Cu_2S) appear (in the field, the conditions are far too oxic and would not favour their precipitation). Dissolved Fe and Cr were omitted from this model for the same reasons already outlined above. At slightly oxidising conditions, native copper (Cu) forms above the sulfate-sulfide boundary but is soon replaced by cuprite (Cu_2O), while malachite ($Cu_2(CO_3)(OH)_2$) develops at higher oxidation potentials; neither cuprite nor native copper were observed in the field. Plotting the water sample of 2013, it manifests itself well within the Cu^{2+} stability field, which means that there should not be any ongoing copper sulfate (i.e., posnjakite) precipitation.

Unfortunately, thermodynamic data for posnjakite ($Cu_4(SO_4)(OH)_6{\cdot}H_2O$), brochantite ($Cu_4(SO_4)(OH)_6$), and many of the other possible secondary copper sulfates (antlerite = $Cu_3SO_4(OH)_4$, langite/wroewolfeite = $Cu_4SO_4(OH)_6{\cdot}2H_2O$, redgillite/montetrisaite = $Cu_6SO_4(OH)_{10}{\cdot}H_2O$) were not available for our modelling (Fatyanov et al., 2000; Bowell and Parshley, 2005; Hammerstrom

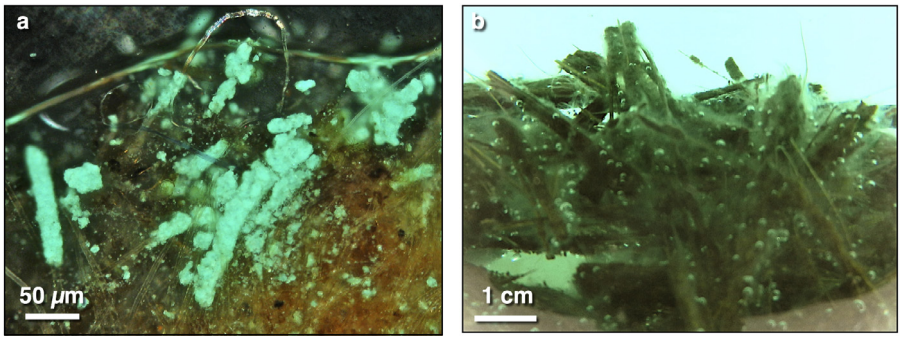

Fig. 6. a Experimentally produced posnjakite coating on cyanobacterial filament. b Oxygen production on cyanobacterial strands is easily observed in the many air bubbles that formed after the experiment was exposed to direct sunlight.

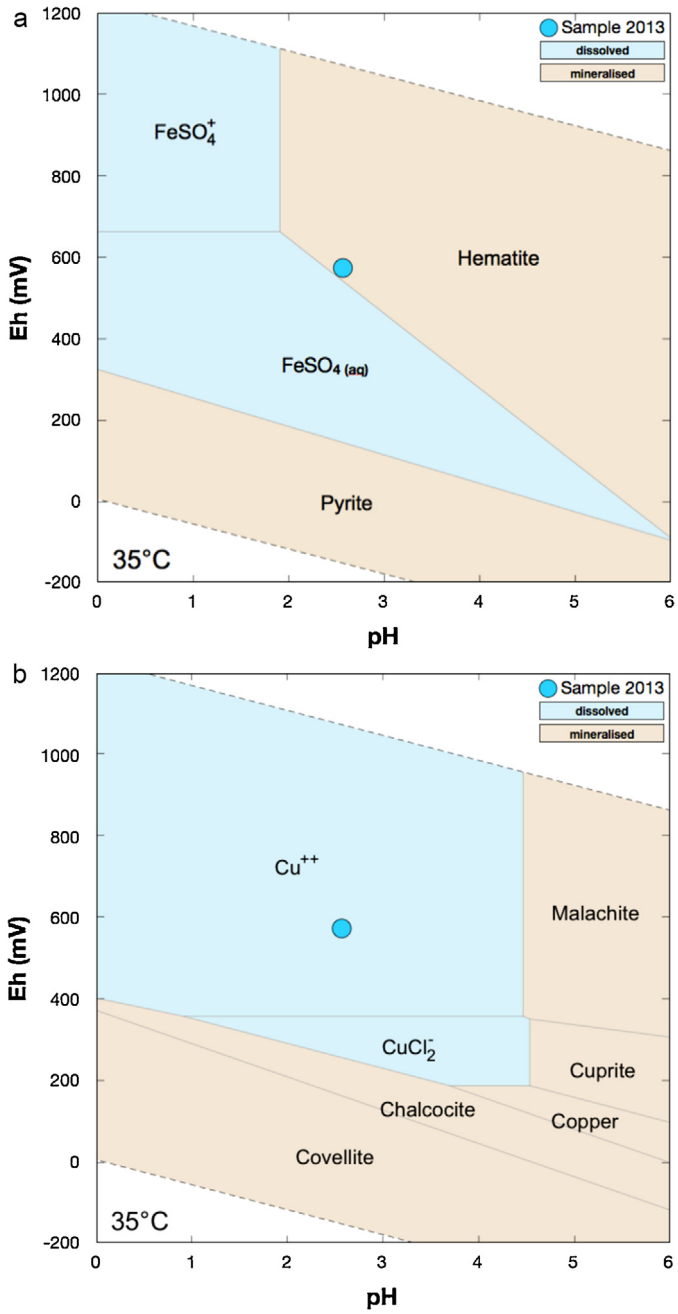

Fig. 7. a Thermodynamic modelling for Fe in the Yanqul mine sump during dry season 2013; standard P (1.013 bar), sampling T = 35.0 °C, assumed concentration $[H_2CO_3/HCO_3^-] = 10^{-3}$ Mol/l; measured concentrations: $[Fe^{2+}] = 10^{-3.66}$ Mol/l, $[Mn^{2+}] = 10^{-3.54}$ Mol/l, $[Zn^{2+}] = 10^{-2.92}$ Mol/l, $[Ni^{2+}] = 10^{-5.49}$ Mol/l, $[SiO_{2(aq)}] = 10^{-3.4}$ Mol/l, $[Cl^-] = 10^{-1.61}$ Mol/l, $[SO_4^{2-}] = 10^{-1.87}$ Mol/l. Although measured, Cu and Cr were not included in this model (see text for explanation), while Mn, Ni, Zn, Si did not have an effect in the shown pH range. Blue stability fields represent dissolved species, light brown fields denote minerals. This diagram was produced with the subroutine Act2 from "The Geochemist's Workbench 8.0" (Bethke, 2008). b Thermodynamic modelling for Cu in the Yanqul mine sump during dry season 2013; standard P (1.013 bar), sampling T = 35.0 °C, assumed concentration $[H_2CO_3/HCO_3^-] = 10^{-3}$ Mol/l; measured concentrations: $[Cu^{2+}] = 10^{-2.42}$ Mol/l, $[Mn^{2+}] = 10^{-3.54}$ Mol/l, $[Zn^{2+}] = 10^{-2.92}$ Mol/l, $[Ni^{2+}] = 10^{-5.49}$ Mol/l, $[SiO_{2(aq)}] = 10^{-3.4}$ Mol/l, $[Cl^-] = 10^{-1.61}$ Mol/l, $[SO_4^{2-}] = 10^{-1.87}$ Mol/l. Although measured, Fe and Cr were not included in this model (see text for explanation), while Mn, Ni, Zn, Si did not have an effect in the shown pH range. Blue stability fields represent dissolved species, light brown fields denote minerals. This diagram was produced with the subroutine Act2 from "The Geochemist's Workbench 8.0" (Bethke, 2008). (For interpretation of the references to colour in this figure legend, the reader is referred to the web version of this article.)

et al., 2005; Laux et al., 2005; Pluth et al., 2005; McDonald and Chao, 2007; Lattanzi et al., 2008; Orlandi and Bonaccorsi, 2009), but most of these minerals were neither found in the field nor formed in experiments. Nevertheless, according to Zittlau et al. (2013), the brochantite stability field largely overlaps with the field of malachite and it can be assumed that the stability of posnjakite is somehow similar to that of brochantite (compare compositions); the discussion below will follow this reasoning.

4. Interpretation and discussion

Examining the element concentrations of the wet and dry seasons, Fe^{2+} and Cu^{2+} clearly stand out with a depression in the overall line pattern for the wet season when the sump waters cooled and were diluted by the influx of rain/ground water (compare Fig. 5). This means that precipitation effects were more effective than during extreme hot climatic conditions, which seems to be surprising

in view of the high metal concentrations. However, with respect to iron, such deposition may already be triggered by a temperature drop, as observed right after the low pH sample returned to the cool lab (~20 °C), where iron hydroxides quickly started to flocculate from the fluid (reflecting a high Fe^{2+} load, despite the fairly high Eh of the field). Hematitic red muds (Fe_2O_3-rich) also bear witness of a widespread precipitation on the quarry floor (earlier than gypsum formation). The copper depression seen in Fig. 5 for the wet season, on the other hand, may indicate more suitable conditions for the microbes to thrive and, thus, a higher metabolic activity with the linked posnjakite precipitation. Having seen that posnjakite coats microbial filaments and covers the surface layer of the chemical sediments in the pond at conditions that should favour dissolved copper species (particularly Cu^{2+}), while it is only present in traces along the edge of the mine sump where brochantite-malachite-dominate, it is obvious that posnjakite must be a metastable precursor to brochantite in the Cu-S-H_2O system, before ageing sets in (Marani et al., 1995; Zittlau et al., 2013).

Therefore, the prevailing (bio-)physicochemical conditions seem to very tightly control this fairly limited mineral association. This impression is supported by the observations of Watanabe et al. (2003), who described mineralised cyanobacterial mats (although different species) carrying various copper minerals, such as woodwardite ($Cu_4Al_2(SO_4)(OH)_{12}\cdot 2\text{-}4H_2O$), dioptase ($CuSiO_2(OH)_2$), and shattuckite ($Cu_5(SiO_3)_4(OH)_2$), in a completely different geochemical environment. These minerals precipitated from solutions which contained much less Cu (~1‰ when compared with the fluids at Yanqul), probably much higher silica levels (seeing the two siliceous compounds) and, judging from the reported pH between 6.0 and 6.6, much lower sulfate concentrations (Si and sulfate were not reported, but a high sulfate content would have reflected sulfide oxidation processes delivering H_2SO_4 into the waters and rendering them much more acidic).

The fact that relatively large quantities of gypsum ($CaSO_4\cdot 2H_2O$) were observed both in the field and in the evaporating fluid from the dry season (in the lab), initially points to competing systems of Ca, Cu, and Fe sulfate formation (natrojarosite ($NaFe_3(SO_4)_2(OH)_6$) was also found on a quarry surface well above the present water level). If Ca (and Fe) consumed all SO_4^{2-} in the pond, posnjakite would not develop. However, field evidence shows that gypsum disappears from the diluted waters of the wet season while, as mentioned above, posnjakite seems to preferentially form during the wet season (probably microbially stabilised during the dry season within the sump). Thus, SO_4^{2-} may partially be swapped between gypsum and posnjakite, effectively buffering the sulfate concentrations.

Among some 40 secondary minerals that have been identified from the Yanqul mining site (and a few more from other locations in northern Oman), posnjakite is a very rare mineral phase that has only been observed in association with microbial growth, while there is not much evidence so far for microbial activity in most of the other products (except for iron oxihydroxides). Viewed in this context, posnjakite precipitation under the climatic conditions of Oman only seems to commence through microbial support.

5. Conclusions

At present, we cannot exclude *Herminiimonas arsenicoxydans* from a possible participation in the mineralisation process by supporting the main "players" while gaining metabolic products (oxygen, nutrients) from the cyanobacteria in parallel; comparable relationships have been observed by Stuetz et al. (1996 and others. However, there is not yet any evidence for an involvement of this bacterium in the posnjakite formation and we conclude that it is the cyanobacteria that force posnjakite precipitation. These microbes also have a considerable potential for mine effluent remediation, especially in fluids with lower Cu concentrations.

Declaration of interest

There is no actual or potential conflict of interest

Acknowledgements

We are obliged to Mr. Saif Khalifah Al-Aamri, formerly manager of business development and exploration (Oman Mining Company L.L.C) for his kind support in accessing the Yanqul site, to Mr. Haitham Al-Fars for his on-site assistance, and to Mr. Saif Al-Mamari of the Central Analytical Research Unit (CAARU) at Sultan Qaboos University, Muscat/Oman for his help with X-ray diffraction, SEM, and EDS analyses. This research did not receive any grant from funding agencies in the public, commercial, or not-for-profit sectors.

References

Abinaya, C., Marikkannan, M., Manikandan, M., Mayandi, J., Suresh, P., Shanmugaiah, V., Ekstrum, C., Pearce, J.M., 2016. Structural and optical characterization and efficacy of hydrothermal synthesized Cu and Ag doped zinc oxide nanoplate bactericides. Mater. Chem. Phys. 184, 172–182.

Anderson, R.T., Lovley, D.R., 2002. Microbial Redox Interactions with Uranium an Environmental Perspective.

Averhoff, B., Müller, V., 2010. Exploring research frontiers in microbiology: recent advances in halophilic and thermophilic extremophiles. Res. Microbiol. 161, 506–514.

Béchennec, F. Métour, J. Le Platel, J.P. Roger, J., 1993. Geological map of the Sultanate of Oman. Scale 1:1.000.000, with explanatory notes (GIS version).

Bednar, A.J., Garbarino, J.R., Ranville, J.F., Wildeman, T.R., 2005. Effects of iron on arsenic speciation and redox chemistry in acid mine water. J. Geochem Explor. 85, 55–62.

Bethke, C.M., 2008. Geochemical and Biogeochemical Modeling, 2nd edition. Cambridge University Press.

Bowell, R.J., Parshley, J.V., 2005. Control of pit-lake water chemistry by secondary minerals Summer Camp pit, Getchell mine, Nevada. Chem. Geol. 215, 373–385.

Brito, Â., Ramos, V., Mota, R., Lima, S., Santos, A., Vieira, J., Vieira, C.P., Kaštovský, J., Vasconcelos, V.M., Tamagnini, P., 2017. Description of new genera and species of marine cyanobacteria from the Portuguese Atlantic coast. Mol. Phylogenet. Evol. 111, 18–34.

Brookins, D.G., 1988. Eh-pH Diagrams for Geochemistry. Springer-Verlag, Berlin.

Chavéz Jr., W.X., 2000. Supergene oxidation of copper deposits: zoning and distribution copper oxide minerals. SEG Newslett. 41, 9–21.

Cleaves, H.J., Crapster-Pregont, E., Jonsson, C.M., Jonsson, C.L., Sverjensky, D.A., Hazen, R.A., 2011. The adsorption of short single-stranded DNA oligomers to mineral surfaces. Chemosphere 83, 1560–1567.

Corenblit, D., Baas, A.C.W., Bornette, G., Darrozes, J., Delmotte, S., Francis, R.A., Gurnell, A.M., Julien, F., Naiman, R.J., Steiger, J., 2011. Feedbacks between geomorphology and biota controlling earth surface processes and landforms: a review of foundation concepts and current understandings. Earth Sci. Rev. 106, 307–331.

Courtin-Nomade, A., Grosbois, C., Marcus, M.A., Fakra, S.C., Beny, J.-M., Foster, A.L., 2009. The weathering of a sulfide orebody: speciation and fate of some potential contaminants. Can. Mineral. 47, 709–724.

Díaz-Tena, E., Rodríguez-Ezquerro, A., López de Lacalle Marcaide, L.N., Gurtubay Bustinduy, L., Elías Sáenz, A., 2013. Use of extremophiles microorganisms for metal removal. Procedia Eng. 63, 67–74.

Davies, H., Weber, P., Lindsay, P., Craw, D., Peake, B., Pope, J., 2011. Geochemical changes during neutralisation of acid mine drainage in a dynamic mountain stream, New Zealand. Appl. Geochem. 26, 2121–2133.

Dekov, V.M., Bindi, B., Burgaud, G., Petersen, S., Asael, D., Rédou, V., Fouquet, Y., Pracejus, B., 2013. Inorganic and biogenic as-sulfide precipitation at seafloor hydrothermal fields. Mar. Geol. 342, 28–38.

Douglas, S., 2004. Microbial biosignatures in evaporite deposits: evidence from death valley, California. Planet. Space Sci. 52, 223–227.

Edraki, M., Golding, S.D., Baublys, K.A., Lawrence, M.G., 2005. Hydrochemistry, mineralogy and sulfur isotope geochemistry of acid mine drainage at the Mt. Morgan mine environment Queensland, Australia. Appl. Geochem. 20, 789–805.

Engel, W., 1953. Untersuchungen über die Kieselsäureverbindungen im Roggenhalm. Planta 41, 358–390.

Essalhi, M., Sizaret, S., Barbanson, L., Chen, Y., Lagroix, F., Demory, F., Nieto, J.M., Sáez, R., Capitán, M.A., 2011. A case study of the internal structures of gossans and weathering processes in the Iberian Pyrite Belt using magnetic fabrics and paleomagnetic dating. Miner. Deposita 46, 981–999.

Fatyanov, A.V., Yurgenson, G.A., Glotova, Y.V., 2000. Effect of the features of the mineral composition and conditions of formations of oxidized copper ores of the Udokan deposit on their beneficiation technology. J. Min. Sci. 36, 185–193.
Frost, R.L., Xi, Y., Palmer, S.J., 2011. The structure of the mineral leogangite $Cu_{10}(OH)_6(SO_4)(AsO_4)_4{\cdot}8H_2O$. Implications for arsenic accumulation and removal. Spectrochim. Acta Part A, 221–227.
Galley, A.G., Hannington, M.D., Jonasson, I.R., 2007. Volcanogenic massive sulphide deposits. In: Goodfellow, W.D. (Ed.), Mineral Deposits of Canada: A Synthesis of Major Deposit Types, District Metallogeny, the Evolution of Geological Provinces, and Exploration Methods. Geological Association of Canada, Mineral deposits devision, Special publication, pp. 141–161.
Genuário, D.B., Dini Andreote, A.P., Vieira Vaz, M.G.M., Fiore, M.F., 2017. Heterocyte-forming cyanobacteria from Brazilian saline-alkaline lakes. Mol. Phylogenet. Evol. 109, 105–112.
Greenwood Hansma, H., 2010. Possible origin of life between mica sheets. J. Theor. Biol. 266, 175–188.
Hammerstrom, J.M., Seal, R.R., Meier, A.L., Kornfeld, J.M., 2005. Secondary sulfate minerals associated with acid drainage in the eastern US: recycling of metals and acidity in surficial environments. Chem. Geol. 215, 407–431.
Hannington, M., 1993. The formation of atacamite during weathering of sulfides on the modern seafloor. Can. Mineral. 31, 945–956.
Hazen, R.M., Ferry, J.M., 2010. Mineral evolution: mineralogy in the fourth dimension. Elements 6, 9–12.
Heinen, W., 1965. Siliciumstoffwechsel bei mikroorganismen. VII. Verteilung der Kieselsäure in Zell-Fraktionen von *Proteus mirabilis* und der Nachweis von Kohlenhydrat-Kieselsäure-Esthern. Arch. Microbiol. 52, 69–79.
Holzapfel, L., Engel, W., 1954. Der Einfluß organischer Kieselsäureverbindungen auf das Wachstum von Aspergillus niger and Tritikum. Z. Naturforsch. 93, 602–606.
Jiang, S.-D., Yao, Q.-Z., Ma, Y.-F., Zhou, G.-T., Fu, S.-Q., 2015. Phosphate-dependent morphological evolution of hydroxyapatite and implication for biomineralisation. Gondwana Res. 28, 858–868.
Jiang, X.D., Sun, X.-M., Guan, Y., Gong, J.-L., Lu, Y., Lu, R.-F., Wang, C., 2017. Biomineralisation of the ferromanganese crusts in the Western Pacific Ocean. J. Asian Earth Sci. 136, 58–67.
Juniper, S.K., Fouquet, Y., 1988. Filamentous iron-silica deposits in modern and ancient hydrothermal sites. Can. Mineral. 26, 859–869.
Kretzschmar, M., 1982. Fossil fungi in iron stromatolites from Warstein (Rhenish Massif, Northwestern Germany). Facies 7, 237–260.
Lattanzi, P., Da Pelo, S., Musu, E., Atzei, D., Elsener, B., Fantauzzi, M., Rossi, A., 2008. Enargite oxidation: a review. Earth Sci. Rev. 86, 62–88.
Laux, J.H., Lindenmeyer, Z.G., Guimarães Teixeira, J.B., Neto, A.B., 2005. Ore genesis at the Camaquã copper mine: a neoproterozoic sediment-hosted deposit in Southern Brazil. Ore Geol. Rev. 26, 71–89.
Li, J., Benzerara, K., Bernard, S., Beyssac, O., 2013. The link between biomineralization and fossilization of bacteria: insights from field and experimental studies. Chem. Geol. 359, 49–69.
Longo, L.M., Blaber, M., 2012. Protein design at the interface of the pre-biotic and biotic worlds. Arch. Biochem. Biophys. 526, 16–21.
Marani, D., Patterson, J.W., Anderson, P.R., 1995. Alkaline precipitation and ageing of Cu(II) in the presence of sulfate. Water Res. 29, 1317–1326.
McDonald, A.M., Chao, G.Y., 2007. Martinite, a new hydrated sodium calcium fluorborosilicate species from Mont Sainthilaire, Quebec: description, structure determination and genetic implications. Can. Mineral. 45, 1281–1292.
Oren, A., 1994. The ecology of the extremely halophilic archaea. FEMS Microbiol. Rev. 13, 415–439.
Orlandi, P., Bonaccorsi, E., 2009. Montetrisaite a new hydroxy-hydrated copper sulfate species from Monte Trisa, Vicenza, Italy. Can. Mineral. 47, 143–151.
Pan-Hou, H.K.S., Imura, N., 1981. Role of hydrogen sulfide in mercury resistance determined by plasmid of *Clostridium cochlearium* T-2. Arch. Microbiol. 129, 49–52.
Panda, A.K., Bisht, S.B., Kumar, N.S., Mandal, S.D., 2015. Report from the 10th international congress on extremophiles. Genomics Data 5, 337–339.
Peeples, T.L., 2014. Bioremediation Using Extremophiles. Elsevier Inc.
Pluth, J.J., Steele, I.M., Kampf, A.R., Green, D.I., 2005. Redgillite, $Cu_6(OH)_{10}(SO_4){\cdot}H_2O$, a new mineral from Caldbeck Fells, Cumbria, England: description and crystal structure. Mineral. Mag. 69, 973–980.
Pracejus, B., Halbach, P., 1996. Do marine moulds influence Hg and Si precipitation in the hydrothermal JADE field (Okinawa Trough)? Chem. Geol. 130, 87–99.
Pracejus, B., Moraetis, D., 2015. Environmentally friendly remediation of Cu-rich mine effluents with a bacterial consortium. In: Pracejus, B. (Ed.), The Seventh Environmental Symposium of German-Arab Scientific Forum for Environmental Studies. Sultan Qaboos University, Sultan Qaboos University, Muscat, Oman, pp. 56–57.
Shuster, J., Bolin, T., MacLean, L.C.W., Southam, G., 2014. The effect of iron-oxidising bacteria on the stability of gold (I) thiosulphate complex. Chem. Geol. 376, 52–60.
Stuetz, R.M., Greene, A.C., Madgwick, J.C., 1996. Microalgal-facilitated bacterial oxidation of manganese. J. Ind. Microbiol. 16, 267–273.
Trevors, J.T., 1987. Silver resistance and accumulation in bacteria. Enzyme Microb. Technol. 9, 331–333.
Vuorinen, A., Hiltunen, P., Hsu, J.C., Tuovinen, O.H., 1983. Solubilization and speciation of iron during pyrite oxidation by *Thiobacillus ferrooxidans*. Geomicrobiol. J. 3, 95–120.
Walter, M.R., Bauld, J., Brock, T.D., 1972. Siliceous algal and bacterial stromatolites in hot spring and geyser effluents of Yellowstone National Park. Science 178, 402–405.
Watanabe, H., Kazue, T., Islam, A.B.M., Khodijah, C.S., 2003. Copper biomineralization with banded structure at Dogamaru mine, Shimane Prefecture, Japan. Res. Pap., 51, ISBN 4-924861-10-3 http://hdl.handle.net/2297/5987.
Wood, J.M., Wang, H.K., 1983. Microbial resistance to heavy metals. Environ. Sci. Technol. 17, 582–590.
Zierenberg, R.A., Schiffman, P., 1990. Microbial control of silver mineralization at a sea-floor hydrothermal site on the northern Gorda Ridge. Nature 348, 155–157.
Zittlau, A.H., Shi, Q., Boerio-Goates, J., Woodfield, B.F., Majzlan, J., 2013. Thermodynamics of the basic copper sulfates antlerite, posnjakite, and brochantite. Chem. Erde 73, 39–50.